Control of pre-rift lithospheric structure on the architecture and evolution of continental rifts: insights from the Main Ethiopian Rift, East Africa

Giacomo Corti[1], Paola Molin[2], Andrea Sembroni[2], Ian D. Bastow[3], Derek Keir[4,5]

1. Consiglio Nazionale delle Ricerche, Istituto di Geoscienze e Georisorse, Via G. La Pira, 4, 50121 Florence, Italy
2. Università degli Studi di Roma Tre, Dipartimento di Scienze, Largo San Leonardo Murialdo, 1, 00146 Roma, Italy
3. Department of Earth Science and Engineering, Imperial College London, London, SW7 2AZ, U.K.
4. Ocean and Earth Science, University of Southampton, Southampton, SO14 3ZH, U.K.
5. Dipartimento di Scienze della Terra, Università degli Studi di Firenze, via G. La Pira 4, 50121 Florence, Italy

Abstract

We investigate the along-axis variations in architecture, segmentation and evolution of the Main Ethiopian Rift (MER), East Africa, and relate these characteristics to the regional geology, lithospheric structure and surface processes. We first illustrate significant along-axis variations in basin architecture through analysis of simplified geological cross-sections in different rift sectors. We then integrate this information with a new analysis of Ethiopian topography and hydrography to illustrate how rift architecture (basin symmetry/asymmetry) is reflected in the margin topography and has been likely amplified by a positive feedback between tectonics (flexural uplift) and surface processes (fluvial erosion, unloading). This analysis shows that ~70% of the 500 km-long MER is asymmetric, with most of the asymmetric rift sectors being characterized by a master fault system on the eastern margin. We finally relate rift architecture and segmentation to the regional geology and geophysical constraints on the lithosphere. We provide strong evidence that rift architecture is controlled by the contrasting nature of the lithosphere beneath the homogeneous, strong Somalian Plateau and the weaker, more heterogeneous Ethiopian Plateau, differences originating from the presence of pre-rift zones of weakness on the Ethiopian Plateau and likely amplified by surface processes. The data provided by this integrated analysis suggest that asymmetric rifts may directly progress to focused axial tectonic-magmatic activity, without transitioning into a symmetric rifting stage. These observations have important implications for the asymmetry of continental rifts and conjugate passive margins worldwide.

This article has been accepted for publication and undergone full peer review but has not been through the copyediting, typesetting, pagination and proofreading process which may lead to differences between this version and the Version of Record. Please cite this article as doi: 10.1002/2017TC004799

Key points

- Structural and geomorphological analysis constrain variations in architecture, segmentation and evolution of the Main Ethiopian Rift
- More than half of the rift is asymmetric, with architecture and segmentation primarily controlled by the pre-rift lithospheric structure
- Asymmetric rifts directly progress to focused axial tectonic-magmatic activity, without transitioning into a symmetric rifting stage

1. Introduction

Continental rifts often have considerable along-strike variations in architecture and magmatism. Variations in fault pattern and evolution may be the result of variations in pre-existing lithospheric rheology, rift width, as well as extension rate and kinematics (e.g., Ebinger, 2005; Ziegler and Cloetingh, 2004; Corti, 2012; Brune, 2016). Along-axis differences in magmatism are commonly explained by processes such as variable mantle potential temperature, heterogeneous anomalous volatile content in the asthenosphere, variable extension rate or processes such as melt focusing at steep gradients of the lithosphere-asthenosphere boundary (e.g., Keir et al., 2015 and references therein). Among these parameters, pre-existing plate structure is expected to play a major role in controlling continental rift architecture, because variations in crustal and lithospheric vertical layering and strength and/or the presence of inherited heterogeneities may significantly influence the style and distribution of deformation at both local and regional scale (e.g., Ziegler and Cloetingh, 2004; Sokoutis et al., 2007; Corti, 2012; Brune, 2016). Continental rifting results from the application of extensional stresses to a pre-deformed, anisotropic lithosphere and, consequently, rift structures are not randomly distributed. They instead tend to follow the trend of pre-existing weaknesses (such as ancient orogenic belts), avoiding stronger regions such as cratons (e.g., Dunbar and Sawyer, 1989; Versfelt and Rosendahl, 1989; Vauchez et al., 1997; Tommasi and Vauchez, 2001; Ziegler and Cloetingh, 2004; Buiter and Torsvik, 2014). In these conditions, variations in the mechanical properties of the rifting plate (e.g., Scholz and Contreras, 1998) and/or the presence of the pervasive and/or discrete fabrics (e.g., Versfelt and Rosendahl, 1989; Ring, 1994) may exert a primary control on the extension-related pattern of faulting at both regional and local scale (e.g., Ziegler and Cloetingh, 2004; Corti, 2012; Brune, 2016). Recent studies support the strong influence played by along-axis

variations in basement fabrics on rift segmentation, inducing significant variations in the characteristics of the rift margins (e.g., vertical throw on major boundary faults) and the symmetry or asymmetry of the rift basins (see for instance examples from Lake Malawi in Lao-Davila et al., 2015 or from the Upper Rhine Graben in Grimmer et al., 2017). Differences in rift symmetry/asymmetry are also typically interpreted to be time-dependent: observations from the East African Rift System suggest a progression from asymmetric to symmetric rifting, eventually followed by axial focusing of the volcanism and faulting (e.g., WoldeGabriel et al., 1990; Hayward and Ebinger, 1996). Moreover, numerical modeling indicates that unloading related to fluvial incision enhances the flexural uplift at major rift escarpments, generating a positive feedback between tectonics and surface processes (Tucker and Slingerland, 1994; Kooi and Beaumont, 1994; Petit et al., 2007). Therefore the dynamic coupling between flexural uplift and fluvial erosion may significantly influence the symmetric or asymmetric structure of the rift.

In this contribution, we integrate detailed geological-structural and geomorphological analysis to investigate the along-axis variations in architecture, segmentation and evolution of the different rift sectors of the Main Ethiopian Rift (MER), East Africa, and relate these characteristics to the lithospheric structure and surface processes. The MER is a classical example of continental rifting developed within a highly anisotropic lithosphere that has experienced several tectonic events over the last one billion years of geological history and tectonics (e.g., Abbate et al., 2015). It is an ideal study locale for the analysis of rift structure in conjunction with surface processes since the expression of different stages in the evolutionary rift sequence, from initial rifting in the south to incipient break-up in the north, are all subaerially exposed and rigorously studied at depth using geophysical techniques (e.g., Corti, 2009; Keir et al., 2013; Ebinger et al., 2017). To investigate the variations in the characteristics of rifting in the MER, we first illustrate simplified geological cross-sections in different portions of the rift, which show significant along-axis variations in the distribution of extension-related deformation and basin architecture. We then use new analysis of the topography and hydrography of the study area as an independent analysis of basin architecture, and to further investigate quantitatively the erosion-tectonics feedback and the response of surface processes to the variable rift architecture along the MER. We relate rift architecture and segmentation to the pre-rift rheology of the continental lithosphere and demonstrate a significant correlation between asymmetry (presence of half graben) of the MER and locally weak lithosphere on the side of the rift lacking a main border fault. We interpret an important influence exerted by the contrasting (pre-rift) nature of the lithosphere

beneath the Ethiopian and Somalian plateaus surrounding the rift valley. We finally show how the data provided by this integrated analysis suggest that rift sectors characterised by an asymmetric architecture can directly progress to focused axial tectono-magmatic activity, without transitioning into a symmetric rifting stage, therefore challenging previous views of evolution of rifting in the East African Rift System (e.g., WoldeGabriel et al., 1990; Hayward and Ebinger, 1996). These observations have important implications for the asymmetry of continental rifts and conjugate passive margins worldwide, which has often been explained in the context of low-angle detachment faults and models involving a lithospheric-scale simple shear deformation (e.g., Wernicke, 1985).

2. Geological setting

The MER, at the northern end of the East African Rift System, accommodates 4-6 mm/yr, N100°E oriented extension between the major Nubia and Somalia Plates (e.g., Saria et al., 2014). This rift is traditionally subdivided into three main sectors, the Southern, Central, and Northern MER (SMER, CMER and NMER, respectively), each differing in terms of fault timing and patterns, and lithospheric characteristics (Fig. 1; e.g., Mohr, 1983; WoldeGabriel et al., 1990; Hayward and Ebinger, 1996; Bonini et al., 2005; Corti, 2009).

The MER sectors are affected by two distinct systems of normal faults: (1) the border faults and (2) a set of faults affecting the rift floor, often referred to as the Wonji Fault Belt (WFB: e.g., Mohr, 1962; Boccaletti et al., 1998). The border faults are long (≥50 km), large-offset (typically >500m) structures that give rise to the major escarpments separating the rift floor from the surrounding plateaus. These faults have been activated diachronously in different rift segments during the last 10-12 Ma (e.g., Balestrieri et al., 2016). Geological data and analysis of the historical and instrumental seismicity suggest that the boundary faults are largely inactive (e.g., Wolfenden et al., 2004; Casey et al., 2006; Keir et al., 2006). Conversely, morphotectonic and geological analysis and Global Positioning System (GPS) data indicate that these faults still accommodate significant extension in the CMER and SMER (Gouin, 1979; Keir et al., 2006; Pizzi et al., 2006; Agostini et al., 2011a; Kogan et al., 2012; Molin and Corti, 2015).

The WFB is an axial tectono-volcanic system characterized by relatively short (typically <20km-long), closely spaced, active faults that exhibit minor vertical throw (typically <100m) with associated extension fractures and grabens (e.g., Boccaletti et al., 1998; Acocella et al., 2003). These faults, which are intimately associated with intense Quaternary-Recent magmatism of the rift floor, developed in the last 2 Ma (e.g. Boccaletti et al., 1998;

Ebinger and Casey, 2001). The WFB is well expressed in the NMER, where its structures form clearly-defined right-stepping en-echelon segments obliquely cutting the rift floor (Ebinger and Casey, 2001). The abundance of Wonji faults decreases southwards: these faults are in an incipient stage of development in the CMER, but practically negligible in the SMER (Fig. 1; e.g., Agostini et al., 2011b).

Along the MER, Quaternary-Recent volcanism is dominated by rhyolites, ignimbrites, pyroclastic deposits, and subordinate basalts (e.g., WoldeGabriel et al., 1990). In the NMER, this activity is strongly focused within the axial WFB (e.g., Ebinger and Casey, 2001). Geophysical data indicate that extension is currently accommodated via a combination of magma intrusion and normal faulting (e.g., Mackenzie et al., 2005; Keranen et al., 2004; Keir et al., 2006), with magma intrusion modifying the composition and thermal structure of the crust and lithosphere beneath the WFB (e.g. Beutel et al., 2010; Daniels et al., 2014). Magmatic modification of the crust/mantle lithosphere and Quaternary-Recent volcanism decreases southwards. In the SMER, consistent with a limited volcano-tectonic activity within the rift, the albeit-sparse geophysical data indicate the absence of significant magmatic modification of the crust/lithosphere (Dugda et al., 2005; Daly et al., 2008).

Overall, these along-axis variations of the distribution and characteristics of the tectono-magmatic activity have been interpreted to reflect a transition from initial rifting in the SMER, with marginal deformation and fault-dominated rift morphology, to advanced rifting stages in the NMER, where prominent axial intrusion, dyking and associated normal faulting testify a phase of magma-assisted rifting during the late stages of continental rifting (e.g., Kendall et al., 2005).

Geophysical studies in the MER suggest that rift location and initial evolution has been controlled by a NE-SW- to N-S-trending lithospheric-scale pre-existing heterogeneity (e.g., Gashawbeza et al., 2004; Bastow et al., 2005, 2008; Keranen and Klemperer, 2008; Keranen et al., 2009; Cornwell et al., 2010), which largely controlled the trend of the Cenozoic rift faulting (e.g., Mohr, 1962; Kazmin et al., 1980). This pre-existing heterogeneity corresponded to a suture zone which separated two distinct Proterozoic basement terranes beneath the Ethiopian and Somalian plateaus (e.g., Vail, 1983; Berhe, 1990; Stern et al., 1990; Stern, 2002; Abdelsalam and Stern, 1996). Extension occurred at approximately the same time as, and after, hotspot-related flood basalt volcanism (Wolfenden et al., 2004), possibly connected to the African Superplume found in the lower mantle beneath southern Africa (e.g., Ritsema et al., 1999). The reactivation of the pre-existing heterogeneity is interpreted to have occurred at the eastern edge of the upwelling mantle not above its centre

(e.g., Bastow et al., 2008), as documented in other flood basalt provinces (Courtillot et al., 1999) and suggested by theoretical modeling (Tommasi and Vauchez, 2001).

Several tectonic events affected Ethiopia prior to the Cenozoic rifting, from collision during the Precambrian to Mesozoic extension (Abbate et al., 2015 and references therein). This long pre-Cenozoic history of tectonic events created pre-existing heterogeneities with variable orientation that have controlled the development of the East African Rift System in Ethiopia (e.g., Korme et al., 2004). At a regional scale, for instance, large-scale E-W or WNW-ESE heterogeneities have controlled the development of major transversal volcano-tectonic lineaments (such as the Yerer-Tullu Wellel Volcanic Lineament: YTVL and the Goba-Bonga; Fig. 1) affecting the rift and the surrounding plateaus (e.g., Abebe Adhana, 2014 and references therein) and marking the transition between the different MER sectors. At a more local scale, pre-existing basement fabrics may have controlled fault and volcanic edifice geometries (e.g., Corti, 2009 and references therein).

3. Methods and results

3.1 Structural cross-sections in the different MER segments

Simplified geological profiles across different sectors of the MER are illustrated in Fig. 2. In these, the subsurface geology and the resulting basin architecture are derived from published cross-sections, extrapolation of surface geology or available subsurface data (see list of references in the caption of Fig. 2). Faults are differentiated based on their exposed minimum vertical displacement (e.g., Lao-Davila et al., 2015), a value that underestimates the actual fault motion since other processes (e.g., erosion, deposition) likely altered the topography of the plateaus and the rift floor (see below). Henceforth, we use the term 'rift symmetry' when the cumulative exposed minimum vertical displacement on major boundary faults is similar on both rift margins, and the term 'rift asymmetry' when this value is significantly lower on one margin with respect to the other (e.g., Lao-Davila et al., 2015). This classification is supported by basin architecture derived from the above-mentioned analysis.

- Profile 1 crosses the northern portion of the NMER and shows an approximately symmetric rift structure, with major boundary fault systems on both western and eastern margins (Ankober and Arboye, respectively; Fig. 1); the recent tectono-magmatic activity of the WFB is well developed at the rift axis in this area (Fantale-Dofan magmatic segment; e.g., Ebinger and Casey, 2001). The boundary faults are generally interpreted to have been deactivated during the Pleistocene (Wolfenden et

al., 2004; Casey et al., 2006), although the high levels of seismicity recorded in the period 2002-2003 indicates ongoing fault slip along the Ankober border fault system (Keir et al., 2006). However, most active tectonics in the area is believed to be accommodated via a combination of intrusion, dyking and normal faulting within the WFB (Keir et al., 2006). This portion of the rift passes into a more asymmetric rift structure northwards into Afar, with a major escarpment on the western side (Ankober fault system; e.g., Wolfenden et al., 2004).

- Similarly, the southern portion of the NMER (Profile 2) displays a marked asymmetry, with the large offset main boundary fault system on the eastern side (Sire fault system) and the northwestern margin characterised by a faulted flexure (e.g., Wolfenden et al., 2004). The axial portion of the rift is affected by recent tectonic and magmatic activity associated with the WFB (Boseti magmatic segment), which accommodates the largest portion of current plate motion (e.g., Kogan et al., 2012).
- Profile 3 illustrates the across-axis structure of the northern portion of the CMER, which is characterized by a major boundary fault system on the western margin forming the Guraghe escarpment. The opposite side of the rift is marked by the Asela-Sire fault system, whose morphological expression may be at least in part obscured by the prominent Pliocene-Quaternary volcanism of large volcanoes (such as Chilalo) at the rift margin (Fig. 1; e.g., Boccaletti et al., 1999). A general tilting of eastern margin towards the rift axis is observed (e.g., Pizzi et al., 2006; Agostini et al., 2011a); although this tilting may be locally controlled by loading from magma intrusion (Corti et al., 2015), the margin architecture may support a rift asymmetry with master fault on the western side. The recent tectono-magmatic activity is well developed on the WFB close to the Asela margin, east of Lake Ziway; Quaternary-Recent magmatic activity also characterized the western margin on the Silti Debre Zeit alignment, although not associated with surface faulting (e.g., Agostini et al., 2011a). Both the boundary fault systems and the WFB accommodate the recent-current deformation in the area (e.g., Keir et al., 2006; Pizzi et al., 2006; Agostini et al., 2011a; Molin and Corti, 2015).
- Further south, the CMER (Profile 4) presents well-expressed, large boundary faults at Fonko and Langano (e.g., Agostini et al., 2011a), which give rise to a roughly symmetric architecture. The WFB volcano-tectonic activity is developed close to the rift axis, and well expressed by the O'a caldera, now occupied by Lake Shala. Both

the rift margins and the WFB are active in this rift sector, and accommodate the recent-current deformation in the area (e.g., Keir et al., 2006; Agostini et al., 2011a; Molin and Corti, 2015).

- Profile 5 illustrates the SMER north of Lake Abaya, which is an asymmetric structure characterized by a major fault escarpment on the eastern side (Agere Selam escarpment) and a faulted, riftward-dipping monocline at the Soddo margin on the western side (e.g., Corti et al., 2013; Philippon et al., 2014). This latter margin is affected by numerous, closely spaced, small normal faults with associated widespread Pleistocene-Holocene volcanism (Fig. 1). The architecture of faults and the distribution of volcanic vents resemble the tectono-magmatic architecture of the WFB, but magma geochemistry is akin to that of the Silti Debre Zeit volcanic belt. Overall, the current volcano-tectonic activity in the north Abaya region is mostly accommodated at the western margin of the rift; conversely, there is little evidence for significant current tectonic activity on the eastern margin (Rooney, 2010; Kogan et al., 2012; Corti et al., 2013; Philippon et al., 2014).
- Further south (Profile 6) rifting becomes more complex: deformation affects a much wider region and is partitioned between the SMER and the Gofa Basin and Range or Gofa Province (e.g., Ebinger et al., 2000; Philippon et al., 2014 and references therein). The SMER itself is subdivided in two different basins, Chamo and Galana, separated by a prominent basement horst (Amaro Horst). The Galana basin displays a marked asymmetry with a major boundary fault system on the western side, whereas the Chamo basin is more symmetric (Ebinger et al., 1993). The minor basins composing the Gofa Province are generally asymmetric, with a master fault on the western sides (e.g., Ebinger et al. 2000). Recent volcanism is almost absent in these basins, and the current tectonic activity is likely accommodated by large boundary faults of both the SMER (e.g., Kogan et al., 2012; Philippon et al., 2014) and the Gofa Province (e.g., Ebinger et al., 2000; Philippon et al., 2014).

Overall, analysis of these data indicate that the MER displays significant along-axis variations in structure and can be subdivided in different portions characterized by symmetric or asymmetric structure.

3.2 Topography and hydrography patterns

We conduct quantitative analysis of topography and hydrography patterns as an independent test of rift symmetry. The flexural uplift generates topography and, as a consequence, rivers incise, further unloading the footwall and enhancing its isostatic uplift (Tucker and Slingerland, 1994). This positive feedback should increase the possible asymmetry of the rift structure. The role of erosion in shaping topography is considered of first order importance since surface processes exert a control on regional scale phenomena (Tucker and Slingerland, 1994 and references therein), and has been widely explored in orogenic belts (Molnar and England, 1990; Willett, 1999; Willett et al., 2001; Brocklehurst and Whipple, 2002; Burbank, 2002; Stern et al., 2005; Wittman et al., 2007; Champagnac et al., 2009 and references therein) and passive margins (Pazzaglia and Gardner, 1994; Kooi and Beaumont, 1994; Tucker and Slingerland, 1994; Anell et al., 2009). However, little progress has been made to understand such dynamics in the context of extensional tectonics. The works available concentrate mainly on the mechanical unloading due to extension (Weissel and Kerner, 1989; Stern and Brink, 1989; Weissel et al., 1995; Poulimenos and Doutsos, 1997; Mueller et al., 2005; Petit et al., 2007) or on the interaction between surface and large-scale lithosphere processes (Burov and Cloetingh, 1997; Daradich et al., 2003; Huismans and Beaumont, 2005; Pik et al., 2008; Mueller et al., 2009).

In the following sections, we analyze the topography and hydrography of the MER to place fully independent constraints on the symmetry of the rift, and to characterize the major surface processes and to investigate the possible role of erosion in rift architecture and its along-axis variations (Fig. 3). We use NASA's Shuttle Radar Topography Mission (SRTM) digital elevation models, whose ~90 m resolution is suitable for regional analysis.

3.2.1 Swath profiles

To describe and quantify the general topographic trend of the MER and surroundings, we generate six swath profiles coincident with the structural profiles (Figs. 1, 3). They show the trend of maximum, minimum and mean elevation in a single plot (Isacks, 1992; Molin et al., 2004; Ponza et al., 2010). We extract them from the SRTM digital elevation models in GIS environment, sampling topography every 2 km into observation windows 30 km wide. The length of each profile is chosen to represent the MER, as in the structural profiles, but also the surroundings to better show the possible river response to tectonic input. In the swath profiles, in correspondence with each rift margin, we measured the drop in elevation from the highlands to the rift floor and the relative topographic gradient. Since the rift floor is

blanketed by volcanic edifices and deposits, the measurements consider just the topographic expression of the interaction between tectonics, volcanism and surface processes.

Swath profile 1 extends from the Ethiopian Plateau in the NNW to the Somalian Plateau in the SSE (Figs. 3, 4). In the NNW, the trend of mean topography shows the flexural uplift affecting the rift shoulder (2.5-3 km of elevation), as documented by Weissel et al. (1995) and Sembroni et al. (2016b). A similar flexural strain is possibly hidden by the strong fluvial erosion affecting the SSE sector where the Somalian Plateau is limited to a narrow strip of land with a mean elevation of ~2700 m (Figs. 3, 4). The MER appears symmetric, limited on both sides by escarpments with similar height and topographic gradient (Table 1). Profile 1 shows also a large difference (~1000 m) in maximum and minimum topography along the northwestern rift shoulder, indicating high local relief. Molin and Corti (2015) interpreted this as typical of a mature stage of rifting when rift margins are highly incised by a well organized fluvial network composed by concave and steep rivers.

Swath profile 2 is located immediately to the east of Addis Ababa where the roughly E-W trending transverse structures, namely the YTVL (Abebe et al., 1998), separates the NMER and CMER (Philippon et al., 2014). This profile shows the rift as an asymmetric structure (Fig. 4) confirmed also by the large difference in topographic gradient between the western and eastern margins (Table 1): the mean elevation of the Ethiopian Plateau decreases progressively from ~3000 m to <1500 m toward the rift floor in a distance of ~60 km; conversely, the Somalian Plateau is well defined with a maximum almost flat topography attained at 2500 m. Here, the difference in elevation of about 1000 m between maximum and minimum topography evidences a strong incision of the inner portion of the Somalian Plateau. This strongly contrasts with the Ethiopian Plateau, where incision is <500 m.

Swath profile 3 in the CMER shows, on both Ethiopian and Somalian plateaus, a large difference between maximum and minimum topography, i.e. a local relief of ~1000 m. West of the CMER, the Ethiopian Plateau is eroded by the tributaries of the Omo River so that its westernmost portion appears to be separated from the Guraghe structure. East of the CMER, the highlands are poorly eroded except where the valley of the Wabe River is located (Fig. 3). The MER shows an asymmetrical configuration with the Guraghe steep escarpment on the northwestern side (~1500 m in height) and a step-like scarp on the southeastern side where the highest peak corresponds to the Galama Volcanic Range. Such configuration is well described by the differences in rift margin elevation drop and topographic gradient values, being the western margin characterized by much higher values than the eastern one (Table 1).

In Swath profile 4 (southern portion of the CMER; Figs. 3, 4) the mean topography is slightly above 2000 m west of the Omo River valley, but increases (to >2500 m) towards the rift margin. Similarly, the Somalian Plateau is ~2500 m except where volcanoes (Mt Chilke, Mt Kaka, Bale Mts) rise from it. Here the MER presents a nearly symmetrical shape with escarpments ~1000 m high characterized by a similar elevation drop (~900 m on average; Table 1). Such a trend is not confirmed by the topography gradient which is slightly higher in the eastern margin (Table 1). Such discrepancy is related to the different distribution of extension-related deformation on the two margins. Whereas the eastern margin is characterised by a single major fault at the base of the Langano escarpment, the western margin is marked by several normal faults (including the major Fonko Fault and associated synthetic and antithetic subparallel structures) distributed over a wider deformation domain (Figs. 1, 2; Agostini et al., 2011a; Molin and Corti, 2015).

Swath profiles 5 is just south of the boundary between the CMER and SMER, where the E-W Goba-Bonga lineament (Abbate and Sagri, 1980) is located. Here the Ethiopian Plateau is characterized by low elevation (~2000 m) and is deeply incised by the Omo River. At the rift margin, topography decreases progressively towards the rift floor (1500 m). Here the MER appears to be asymmetrical since to the east, by an elevation drop of ~950 m and a topography gradient of 0.067 (Table 1), mean topography increases to >2500 m (Somalian Plateau) and then decreases progressively. Here the Somalian Plateau is strongly incised by fluvial network. To the west the rift margin presents a small elevation drop (665 m) and topography gradient (0.019; Table 1); in this portion there is no morphological evidence of a tectonic escarpment (Fig. 3).

Swath profile 6, across the southernmost portion of the dome-shaped topography, cuts across the complex region of diffuse deformation including the SMER and the Gofa Province (see above). The profile reveals the presence of several tectonic basins mostly west of the MER. Here the MER (corresponding with the Chamo basin) is narrower and symmetrical with both margins standing at a mean elevation of more than 2000 m and presenting similar elevation drop and topography gradient values (Table 1). The topography becomes relatively regular on the southeastern portion (~1500 m in mean elevation) where the profile crosses the Precambrian rocks standing at the periphery of the dome-shaped topography relative to the upwelling of the Afar plume (Sembroni et al., 2016a, b and references therein).

3.2.3 Local relief

We constrain a map of local relief of the study area to quantify the difference in elevation between valley bottoms and peaks, and to investigate the spatial distribution of river incision. In detail, we smooth the maximum and minimum topography of the SRTM digital elevation models by a 10 km diameter circular moving window (low-pass filter) in GIS environment. We choose such a value since it is the average spacing of the main valleys (7^{th} Strahler order with respect to a critical drainage area of ~4 km^2). This allows the removal of small valleys, highlighting the regional-scale features. The results of the smoothing are two surfaces: the sub-envelope surface, which describes the general pattern of valley bottoms elevations, and the envelope surface, that connects peaks elevations. We obtain the local relief map by arithmetically subtracting the resulting surfaces (Fig. 5a). To demonstrate better the relationship between topography and river incision, we extract 6 swath profiles across the local relief map. In more detail, using the same observation windows of Fig. 3, we sample the local relief along 5 profiles and calculate the mean local relief value. The results are plotted in Fig. 4 to facilitate the comparison between the trend of local relief and the topography configuration.

The study area is characterized by a general low local relief (<300 m) with the lowest values concentrated in the MER and the portions of the Ethiopian and Somalian plateaus preserved by erosion (Fig. 5a). Such features represent the ancient top surface of the Trap deposits and have been used by some authors to calculate the volume and thickness of flood basalts (Gani et al., 2007; Sembroni et al., 2016b) and to reconstruct the post-Trap topography (Sembroni et al., 2016b). Values >300 m are in the MER where volcanoes and active tectonics cause the increase of local relief up to 600 m (Figs. 4, 5a). Values >300 m characterize also the inner sectors of the Ethiopian and Somalian plateaus, where rivers incised deep canyons, and the rift margins (Figs. 4, 5a). Here the relief increases where the extensional tectonics generates escarpments and possibly a flexural uplift of the footwall (Sembroni et al., 2016b). Indeed, relatively high values of local relief are at the footwall of the major border faults, further evidence for the symmetric or asymmetric structure of the rift (Figs. 4, 5a).

The topography configuration is much more complicated in the southernmost sector of the MER where several tectonic basins as well as the strong incision of the Omo River make difficult the reading of the local relief map (Figs. 4, 5a).

3.2.4 k_{sn} map

Since hydrography is sensitive to local and regional tectonic inputs (e.g., Pazzaglia et al., 1998; Wegmann and Pazzaglia, 2002; Tomkin, et al., 2003; Lock et al., 2006; Wobus et al., 2006; Scotti et al., 2013; Molin and Corti, 2015; Sembroni et al., 2016a), we investigate the MER drainage system focusing on the channel steepness variation.

To study river incision both at steady- and transient-state, a power law is widely used which relates channel slope *S* and drainage area *A* (Hack, 1957; Flint, 1974; Howard et al., 1994; Sklar and Dietrich, 1998; Whipple and Tucker, 1999; Snyder et al., 2000; Whipple et al., 2000; Schorghofer and Rothman, 2002; Kobor and Roering, 2004):

$$S = k_s A^{-\theta}, \quad (1)$$

where k_s and θ are the steepness and concavity indices. Several studies evidence a positive correlation between steepness index and uplift rate, although it is strongly influenced by geologic setting and climate (e.g., Snyder et al., 2000; Kirby and Whipple, 2001; Whipple, 2004; Wobus et al., 2006; Kirby et al., 2007; Molin and Corti, 2015). Under steady-state conditions, the θ=0.4-0.6, but theoretically ~0.45 (Tarboton et al., 1989; Whipple and Tucker, 1999; Snyder et al., 2000; Kirby and Whipple, 2001; Whipple, 2004; Whipple et al., 2007). This theoretical value is used as a reference concavity to normalize the steepness index (k_{sn}; Wobus et al., 2006). This allows the comparison of rivers regardless the size of the drainage basins. To reveal the general variation in steepness index values along river courses, we extract the map of the along channel variation in k_{sn} by using the Stream Profiler tool developed by Whipple et al. (2007); the critical drainage area is set at 10^7 m^2 to obtain a detailed analysis of the river network up to the 3th Strahler order. Once obtained, the linear shape file has been converted into a point shape file and interpolated by a nearest neighbour triangulation algorithm to extract the areal distribution of k_{sn}.

To show the pattern of k_{sn} with respect to topography, we extract 6 swath profiles across the k_{sn} map. Using the same observation windows as Fig. 3, we sample the k_{sn} map along 5 profiles and calculate the mean value. The results are plotted in Fig. 4 to compare the channel steepness trend with the topography pattern. Since the channel steepness is very sensitive also to very small variation in slope, both map and profiles show abrupt changes in values on short distance.

The k_{sn} map (Fig. 5b) shows a correspondence between high values of k_{sn} (> 350, which coincide with knickpoints and knickzones) and rock type changes, especially along the

Ethiopian and Somalian plateaus scarps. Medium-high values (>200) correspond to the rift margins (Figs. 4, 5b) where the tectonic structures have generated knickpoints and knickzones (Molin and Corti, 2015). At the footwall of the major border faults of MER, higher values of k_{sn} evidence the symmetric or asymmetric structure of the rift (Figs. 4, 5b).

4. Discussion

We have used structural, topographic and hydrographic analysis to constrain the architecture and segmentation of the MER, considering the interaction between tectonics and fluvial erosion and the role of such interaction in dictating the evolution of the rift.

The MER displays significant along-axis structural variation: the MER's three traditional subdivisions, the NMER, CMER and SMER (e.g., Agostini et al., 2011b) can be further subdivided into portions characterized by symmetric or asymmetric structure (Fig. 6a; Table 1). In general, ~70% of the 500 km-long rift is asymmetric. The symmetry or asymmetry of the rift is reflected in the topography and in the rift margin elevation drop and topography gradient. The tectonic symmetry/asymmetry is supported by the convergence/divergence of such values for both rift margins (Table 1). Where major boundary faults are present, the rift margin reaches higher elevations (Figs. 2, 3, 4), locally showing a decrease at the footwall of the tectonic structures typical of flexural uplift (Sembroni et al., 2016b). This process increases elevation and, therefore, stream power and channel steepness (Fig. 5b), that results in river incision (Fig. 5a). Unloading related to fluvial erosion could have enhanced the flexural uplift, generating a positive feedback between tectonics and surface processes. This dynamic coupling between flexural uplift and fluvial incision probably amplified the symmetric or asymmetric structure of the rift. A similar scarp evolutionary scenario has been predicted by numerical modeling (Tucker and Slingerland, 1994; Kooi and Beaumont, 1994; Petit et al., 2007).

Generally, most of the asymmetric sectors have a master fault system located on the eastern margin. In particular, >70% of the eastern margin is marked by a major boundary fault; the remainder is marked by minor faulting and monoclines. In some cases (e.g., Asela), the margin morphology is masked by prominent recent volcanism, and therefore 70% can be considered a lower bound. Next, we interpret the spatial pattern of border faulting in light of geophysical constraints on lithospheric structure and strength.

4.1 Relations between rift architecture and pre-rift lithospheric rheology

The MER has developed within a region that has experienced several tectonic events, from different phases of collision during the Precambrian to Mesozoic extension (e.g., Chorowitz, 2005), which have resulted in significant lateral variations in the rheological structure of the lithosphere. The rift valley formed within an ancient suture zone sandwiched between two distinct lithospheric domains beneath the Ethiopian and Somalian plateaus (e.g., Vail, 1983; Berhe, 1990; Kazmin et al., 1978; Bastow et al., 2008; Cornwell et al, 2010; Keranen and Klemperer, 2008; see above section 2). Rift architecture and the along-axis structural variations are likely controlled by differences in the crustal/lithospheric structures of these two domains.

Specifically, the eastern margin is characterised by limited along-axis variations in architecture, being dominated by large boundary escarpments along almost its entire length; this likely reflects the strong and homogeneous nature of the lithosphere beneath the Somalian Plateau (e.g., Keranen and Klemperer, 2008). Conversely, the western margin is more irregular, with segments characterised by large boundary faults (Ankober, Fonko-Guraghe, Gamo-Gidole) alternating with segments marked by gentle flexures towards the rift axis. This reflects a more complex structure of the Ethiopian plateau lithosphere, interpreted to comprise two different portions: a strong northern portion, strengthened by cooled (pre-rift) mafic underplate, and a southern portion, with thinner crust and weaker rheology (Fig. 6b; e.g., Keranen and Klemperer, 2008). This southern portion is marked by the presence of two major transversal lineaments, YTVL and Goba Bonga, resulting from the Cenozoic reactivation of pre-existing Neoproterozoic weaknesses, sub-parallel to the trend of the Gulf of Aden (e.g., Abbate and Sagri, 1980; Abebe et al., 1998; Korme et al., 2004; Abebe Adhana, 2014). Where these pre-existing weak heterogeneities intersect at a high angle the rift, the western margin lacks major boundary faults, which are instead replaced by gentle monoclines; this, together with well-developed faults on the eastern side, results in an overall asymmetry of the rift (Fig. 6).

Geophysical analysis of the crust and mantle beneath both plateaus (e.g. Dugda et al., 2005; Whaler et al., 2006; Stuart et al., 2006; Mackenzie et al., 2005; Maguire et al., 2006; Bastow et al., 2008; Keranen et al., 2009) support this interpretation (Fig. 6). Crustal thickness and bulk crustal Vp/Vs ratios are relatively heterogeneous beneath the Ethiopian Plateau (41-43 km in the NW, <40 km in the SW) compared to the homogenous crust (38-40 km thickness, 1.8 Vp/Vs ratio) beneath the Somalian Plateau (Fig. 6b; Stuart et al., 2006; Keranen et al., 2009). The crust beneath the YTVL of the Ethiopian Plateau is characterized by anomalously

high Vp/Vs (1.9-2; e.g., Stuart et al., 2006), which is interpreted as evidence for the presence of melt in the crust. In support of the interpretation of elevated fluid content in the crust beneath the YTVL, magnetotelluric data show low resistivities (~2 Ωm), in contrast to the high resistivities (~100 Ωm) found beneath the Somalian Plateau. Analysis of crustal thickness indicates that the YTVL corresponds to a sharp gradient in Moho depth (Fig. 6b). In particular, this transversal lineament corresponds to the boundary of the strong and thick crust of the northern portion of the Ethiopian Plateau (Keranen and Klemperer, 2008). South of the YTVL, the Ethiopian Plateau (including the Goba Bonga region) has a crust that is significantly thinner than the average crustal thickness of the Ethiopian-Somalian plateaus (see also Keranen et al., 2009). Notably, along-axis variations in crustal thickness in the Ethiopian Plateau match well the subdivision in symmetric or asymmetric rift portions we suggest, with major rift escarpments corresponding to portions characterised by thick (and likely strong) crust (Fig. 6b).

Our interpretation of heterogeneous crustal composition, thickness and strength for the Ethiopian Plateau is supported by geophysical constraints on properties of the whole plate. The 75 km depth slice through relative arrival-time body-wave tomographic model of Bastow et al. (2008) shows distinctive low velocity anomalies that extend from the rift valley to the Ethiopian Plateau in two lobes specifically beneath the YTVL and Goba Bonga transversal lineament (Fig. 6b). These low velocity anomalies are best explained by a combination of a thermal anomaly and partial melting in response to upwelling and decompression of the asthenosphere caused by localized extension and thinning of the lithosphere beneath the two volcanic lineaments (e.g., Bastow et al., 2010; Gallacher et al., 2016). In support of the hypothesis of plate weakening, the values of the effective elastic plate thickness (Te; Pérez-Gussinyé et al., 2009) are generally much lower and more heterogeneous for the Ethiopian Plateau than for the Somalian Plateau, where Te can reach values >60 km. The most prominent asymmetries occur south of Addis Ababa where the Ethiopian Plateau is marked by major E-W trending YTVL and the Bonga Goba transversal lineament. This latter lineament corresponds to a narrow E-W domain where Te decreases to 10-15 km (Pérez-Gussinyé et al., 2009). Whether zones of thinned crust, and inferred thinned lithosphere, beneath the YTVL and the Bonga Goba transversal lineament are directly caused by pre-rift lithospheric thin zones, or by syn-rift extension that exploits pre-rift zones of weakness is impossible to tell. However, both interpretations strongly suggest that pre-rift structural control exerts a significant influence on the current structure of the lithosphere.

In summary, all the above-mentioned observations suggest that, although different processes may have contributed to the present architecture of the MER (e.g., flexure during initial rifting stages, Kazmin et al., 1980; bending related to magma intrusion, Corti et al., 2015; Buck, 2017), the major control has been likely exerted by the different rheological nature of the Ethiopian and Somalian plateaus. This supports recent observations from other continental rifts (e.g., Malawi Rift, Upper Rhine Graben) illustrating that along-axis variations in basement fabric have a strong influence on basin architecture and segmentation as well as on the characteristics of the rift margins (e.g., Lao-Davila et al., 2015; Grimmer et al., 2017).

4.2 General implications for continental rifting and break-up

Overall, our integrated analysis suggests that the MER is characterized by a Mio-Pliocene rift segmentation controlled by the pre-rift lithospheric structure, which results in 80-100 km rift portions characterized by alternating symmetric/asymmetric basins. The timescale (~10 Myrs) of the formation of this architecture is at least partially due to the positive feedback between tectonic and fluvial erosion which emphasizes the flexural uplift of the rift margin faults and its topographic expression. With increasing extension into the Quaternary, the along-rift segmentation of the axis is progressively defined by the 40-60 km long magmatic segments in the NMER (Ebinger and Casey, 2001). This indicates that whereas rift architecture is mostly controlled by the pre-rift lithospheric structure during initial rifting stages, other processes (such as magmatism and rift obliquity; e.g., Corti, 2008) define axial segmentation during more advanced rifting (e.g., Ebinger, 2005).

One important outcome of our work is that there is no evidence for a progressive evolution from asymmetric to symmetric rifting with time, as proposed by previous works (WoldeGabriel etal.,1990; Hayward and Ebinger, 1996). Indeed, asymmetric rifts may be characterized by a direct focusing of the tectonic-magmatic activity at the rift axis, as observed in the NMER (see section 2 in Fig. 2; Ebinger and Casey, 2001; Ebinger, 2005) and supported by modelling of rift evolution (e.g., Corti, 2008). An alternative behaviour has been observed in the northern portion of the SMER, where deformation seems to have transitioned from an asymmetric structure with master fault on the eastern side to localized volcano-tectonic activity at the western margin in the Soddo area (Corti et al., 2013), a process which may have been controlled by localized magma intrusion and a consequent weakening of the local crust/lithosphere.

Such observations have important implications for the asymmetry of conjugate passive margins worldwide. Our data suggest that asymmetry may result from the pre-rift asymmetric nature of the lithosphere, which controls the development of major boundary faults on one side, and controls the less-developed faulting on the opposite side. The influence of the rheological and geometrical characteristics of lithosphere on the asymmetry of a rift system has been evidenced also by numerical models (e.g., Huismans and Beaumont, 2014) indicating that a strong lithosphere supports large flexural stresses that control the flank uplift and, consequently, the erosion rate. Therefore, asymmetry does not require low-angle detachment faults and lithospheric-scale simple shear deformation (e.g., Wernicke, 1985): our data support the high-angle nature of large boundary faults (e.g., Keir et al., 2006), arguing against significant simple shear deformation. The topographic expression of these structures is enhanced by the unloading related to fluvial erosion.

The integrated approach to such a complex context like continental rifting is essential to understand the role of sub-crustal, crustal and surface processes in generating regional scale tectonic structures and relative landscape.

5. Conclusions

In this work, along-axis variations in architecture, segmentation and evolution of the different sectors of the Main Ethiopian Rift (MER), East Africa, have been analysed by means of an integrated structural and geomorphological analysis and compared with regional geology and geophysical constraints on lithospheric structure. This analysis suggests the following main conclusions:

-~70% of the 500 km-long MER is asymmetric, with most asymmetric sectors characterized by a master fault system on the eastern margin. Thus, >70% of the eastern margin is marked by a major boundary fault; the rest is marked by minor faulting and monoclines.

-The symmetry or asymmetry of the rift is reflected in the topography and hydrography. The rift margin topography gradients differ by <40% in the symmetric portions and >100% in the asymmetric ones. Steep rivers deeply incise the footwall of the major border faults; this erosional unloading increases the isostatic uplift of footwall, enhancing the symmetric/asymmetric topography of each sector of the rift.

-Rift architecture and segmentation are strongly controlled by the pre-rift lithospheric structure, especially the contrasting nature of the homogeneous, strong Somalian Plateau and the weaker, more heterogeneous Ethiopian Plateau.

-Asymmetric rift sectors may directly progress to focused axial tectonic-magmatic activity, without transitioning into a symmetric rifting stage.

Acknowledgments

We thank three anonymous reviewers and the Associate Editor Tesfaye Kidane for the detailed comments which helped to improve this manuscript. We also thank Federico Sani for discussions. D.K. is supported by NERC grant NE/L013932/1. The data supporting this paper are listed in the references and available within tables and figures; any further information can be obtained upon request.

References

Abbate, E., and Sagri, M. (1980). Volcanites of Ethiopian and Somali Plateaus and major tectonic lines. Atti Convegni Lincei, 47, 219-227.

Abbate, E., Bruni P., and Sagri, M. (2015). Geology of Ethiopia: A Review and Geomorphological Perspectives. In: P. Billi (ed.), Landscapes and Landforms of Ethiopia, World Geomorphological Landscapes, Springer Science+Business Media, Dordrecht, pp. 33-64.

Abebe Adhana, T. (2014). The occurrence of a complete continental rift type of volcanic rocks suite along the Yerer–Tullu Wellel Volcano Tectonic Lineament, Central Ethiopia. J. Afr. Earth Sci., 99, 374-385.

Abebe T., Manetti P., Bonini M., Corti G., Innocenti F., Mazzarini F., and Pecskay Z. (2005). Geological Map (Scale 1:200 000) of the Northern Main Ethiopian Rift and its implication for the volcano-tectonic evolution of the Rift. Geological Society of America Maps and Charts, MCH094, 20 pp.

Abebe, T., Mazzarini, F., Innocenti, F., and Manetti, P. (1998). The Yerer–Tullu Wellel volcanotectonic lineament: A transtentional structure in Central Ethiopia and the associated magmatic activity, J. Afr. Earth Sci., 26, 135–150.

Abdelsalam, M. G., and Stern, R. J. (1996). Sutures and shear zones in the Arabian-Nubian Shield. J. Afr. Earth Sci., 23, 289-310.

Acocella, V., Korme, T., and Salvini, F. (2003). Formation of normal faults along the axial zone of the Ethiopian rift. J. Struct. Geol., 25, 503–513.

Agostini, A., Bonini, M., Corti, G., Sani, F., and Manetti, P. (2011a). Distribution of quaternary deformation in the central Main Ethiopian Rift, East Africa. Tectonics, 30(4).

Agostini, A., Bonini, M., Corti, G., Sani, F., and Mazzarini, F. (2011b). Fault architecture in the Main Ethiopian Rift and comparison with experimental models: implications for rift evolution and Nubia-Somalia kinematics. Earth Planet. Sci. Letts., 301, 479–492.

Balestrieri, M.L., Bonini M., Corti G., Sani F., and Philippon M. (2016). A refinement of the chronology of rift-related faulting in the Broadly Rifted Zone, southern Ethiopia, through apatite fission-track analysis. Tectonophysics, 671, 42–55.

Bastow, I.D., Stuart, G.W., Kendall, J.M. and Ebinger, C.J. (2005). Upper mantle seismic structure in a region of incipient continental breakup: northern Ethiopian rift. Geophys. J. Int., 162(2), 479–493.

Bastow, I. D., Nyblade, A. A., Stuart, G. W., Rooney, T. O., and Benoit, M. H. (2008). Upper mantle seismic structure beneath the Ethiopian hot spot: Rifting at the edge of the African

low-velocity anomaly. Geochem. Geophys. Geosyst., 9, Q12022, doi:10.1029/2008GC002107.

Bastow, I. D., Pilidou S., Kendall J.-M., and Stuart, G. W. (2010). Melt-induced seismic anisotropy and magma assisted rifting in Ethiopia: Evidence from surface waves. Geochem. Geophys. Geosyst., 11, Q0AB05, doi:10.1029/2010GC003036.

Berhe, S.M. (1990). Ophiolites in northeast and East Africa: Implications for Proterozoic crustal growth. J. Geol. Soc. Lond., 147, 41–57.

Boccaletti, M., Bonini, M., Mazzuoli, R., Abebe, B., Piccardi, L. and Tortorici, L. (1998). Quaternary oblique extensional tectonics in the Ethiopian Rift (Horn of Africa), Tectonophysics, 287, 97-116.

Boccaletti, M., Mazzuoli, R., Bonini, M., Trua, T., and Abebe, B. (1999). Plio-Quaternary volcano-tectonic activity in the northern sector of the Main Ethiopian Rift (MER): relationships with oblique rifting. J. Afri. Earth Sci., 29, 679-698.

Bonini, M., Corti, G., Innocenti, F., Manetti, P., Mazzarini, F., Abebe, T., and Pecskay, Z. (2005). The evolution of the Main Ethiopian Rift in the frame of Afar and Kenya rifts propagation. Tectonics, 24, TC1007, doi:10.1029/2004TC001680.

Brocklehurst, S. H., andWhipple, K. X. (2002). Glacial erosion and relief production in the eastern Sierra Nevada, California. Geomorphology, 42(1), 1-24.

Brune, S. (2016), Rifts and rifted margins: A review of geodynamic processes and natural hazards, edited by J. C. Duarte and W. P. Schellart, Plate Boundaries Nat. Hazards, 11–37, doi:10.1002/9781119054146.ch2.

Buck, W.R. (2017). The role of magmatic loads and rift jumps in generating seaward dipping reflectors on volcanic rifted margins. Earth Planet. Sci. Letts., 466, 62–69.

Buiter, S.J.H. and Torsvik, T.H. (2014). A review of Wilson Cycle plate margins: A role for mantle plumes in continental break-up along sutures? Gondwana Research, 26, 627–653.

Burov, E. andCloetingh, S. A. P. L. (1997). Erosion and rift dynamics: new thermomechanical aspects of post-rift evolution of extensional basins. Earth Planet. Sci. Letts., 150(1-2), 7-26.

Casey, M., Ebinger, C.J., Keir, D., Gloaguen, R., and Mohamad, F. (2006). Strain accommodation in transitional rifts: extension by magma intrusion and faulting in Ethiopian rift magmatic segments. In: Yirgu G., Ebinger C.J., Maguire P.K.H., (Eds), 2006. The Afar Volcanic Province within the East African Rift System. Geol. Soc. Spec. Pub., 259, 143-163.

Champagnac, J. D., Schlunegger, F., Norton, K., von Blanckenburg, F., Abbühl, L. M., and Schwab, M. (2009). Erosion-driven uplift of the modern Central Alps. Tectonophysics, 474(1), 236-249.

Cornwell, D. G., Maguire P.K.H., England R.W., and Stuart G.W. (2010). Imaging detailed crustal structure and magmatic intrusion across the Ethiopian Rift using a dense linear broadband array. Geochem., Geophys., Geosyst. 11, 1, Q0AB03, doi:10.1029/2009GC002637.

Corti, G. (2008). Control of rift obliquity on the evolution and segmentation of the main Ethiopian rift. Nat. Geosci., 1, 258-262.

Corti, G. (2009). Continental rift evolution: from rift initiation to incipient break-up in the Main Ethiopian Rift, East Africa. Earth Science Reviews, 96, 1–53.

Corti, G. (2012). Evolution and characteristics of continental rifting: analogue modeling-inspired view and comparison with examples from the East African Rift System. Tectonophysics, 522-523, 1-33, http://dx.doi.org/10.1016/j.tecto.2011.06.010

Corti, G., Sani, F., Philippon, M., Sokoutis, D., Willingshofer, E., and Molin P. (2013). Quaternary volcano-tectonic activity in the Soddo region, western margin of the Southern Main Ethiopian Rift. Tectonics 32, 861–879

Corti, G., Agostini, A., Keir, D., Van Wijk, J., Bastow, I.D., and Ranalli, G. (2015). Magma-induced axial subsidence during final-stage rifting: implications for the development of seaward dipping reflectors. Geosphere, 11, 563–571, DOI: 10.1130/GES01076.1.

Courtillot, V., Jaupart, C., Manighetti, I., Tapponnier, P., and Besse, J. (1999). On causal links between flood basalts and continental breakup. Earth Planet. Sci. Letts..166, 177–195.

Daly, E., Keir, D., Ebinger, C. J., Stuart, G. W., Bastow, I. D., and Ayele, A. (2008). Crustal tomographic imaging of a transitional continental rift: the Ethiopian rift. Geophys. J. Int., 172, 1033–1048.

Daniels, K. A., Bastow, I. D., Keir, D., Sparks, R. S. J., and Menand, T. (2014). Thermal models of dyke intrusion during development of continent–ocean transition. Earth Planet. Sci. Letts., 385, 145-153. DOI:10.1016/j.epsl.2013.09.018

Davidson, A., compiler (1983). The Omo River project: reconnaissance geology and geochemistry of parts of Illubabor, Kefa, Gemu Gofa, and Sidamo. Ethiopian Institute Geological Surveys Bulletin, 2, 1–89.

Dugda, M.T., Nyblade, A.A., Jordi, J., Langston, C.A., Ammon, C.J. and Simiyu, S. (2005). Crustal structure in Ethiopia and Kenya from receiver function analysis: implications for

rift development in eastern Africa. J. Geophys. Res., 110(B1), B01303, doi:10.1029/2004JB003065.

Dunbar, J.A., and Sawyer, D.S. (1989). Continental rifting at pre-existing lithospheric weaknesses. Nature, 242, 565-571.

Ebinger, C. (2005). Continental breakup: The East African perspective. Astronomy and Geophysics, 46, 2.16-2.21.

Ebinger, C.J. and Casey, M. (2001). Continental breakup in magmatic provinces: An Ethiopian example. Geology 29, 527-530.

Ebinger, C. J., Yemane, T., Harding, D. J., Tesfaye, S., Kelley, S., and Rex, D. C. (2000). Rift deflection, migration, and propagation: Linkage of the Ethiopian and Eastern rifts, Africa. Geological Society of America Bulletin, 112(2), 163-176.

Ebinger, C.J., Yemane, T., WoldeGabriel, G., Aronson, J.L., and Walter, R.C. (1993). Late Eocene-Recent volcanism and faulting in the southern main Ethiopian rift. J. Geol. Soc. Lond. 150, 99-108.

Ebinger, C. J., Keir, D., Bastow, I. D., Whaler, K., Hammond, J. O. S., Ayele, A., Miller, M., Tiberi, C. and Hautot, S. (2017). Crustal structure of active deformation zones in Africa: Implications for global crustal processes. Tectonics, 36, doi:10.1002/2017TC004526.

Ethiopian Mapping Agency (1981). Geological Map of the Ethiopian Rift (scale 1:500.000). Kazmin V., Berhe S.M. (Eds.). Ethiopian Mapping Agency, Addis Ababa, Ethiopia.

Ethiopian Mapping Agency (1981). Geological Map of the Ethiopia, Nazret Sheet. Ethiopian Mapping Agency, Addis Ababa, Ethiopia.

Ethiopian Mapping Authority (1996). Geological Map of Ethiopia (scale 1:2.000.000). Ethiopian Mapping Authority, Addis Ababa, Ethiopia.

Flint, J. J. (1974). Stream gradient as a function of order, magnitude, and discharge. Water Resources Research 10, 969–973.

Gallacher, R. J., Keir, D., Harmon, N., Stuart, G., Leroy, S., Hammond, J. O., ... & Ahmed, A. (2016). The initiation of segmented buoyancy-driven melting during continental breakup. Nature Communications, 7:13110, DOI: 10.1038/ncomms13110

Gani, N.D., Abdelsalam, M.G., and Gani, M.R. (2007). Blue Nile incision on the Ethiopian Plateau: pulsed plateau growth, Pliocene uplift, and hominin evolution. GSA Today 17, 4–11.

Gashawbeza, E.M., S.L. Klemperer, A.A. Nyblade, K.T. Walker, and K.M. Keranen (2004). Shear-wave splitting in Ethiopia: Precambrian mantle anisotropy locally modified by Neogene rifting. Geophysical Research Letters, 31, L18602, doi:10.1029/2004GL020471.

Gouin, P. (1979). Earthquake history of Ethiopia and the Horn of Africa. IDRC, Ottawa, 258 pp.

Grimmer, J. C., Ritter, J. R. R., Eisbacher, G. H., and Fielitz, V. (2017). The Late Variscan control on the location and asymmetry of the Upper Rhine Graben. Int J Earth Sci (Geol Rundsch), 106, 827–853, DOI 10.1007/s00531-016-1336-x.

Hack, J. T. (1957). Studies of longitudinal profiles in Virginia and Maryland. U. S. Geological Survey Professional Paper 294 (B), 45–97.

Hayward, N.J. and Ebinger, C.J. (1996). Variations in the along-axis segmentation of the Afar Rift system. Tectonics, 15, 244-257.

Howard, A.D., Dietrich, W.E., and Seidl, M.A. (1994). Modeling fluvial erosion on regional to continental scales. J. Geophys. Res. Solid Earth 99, 13971–13986.

Huismans, R. S., and Beaumont, C. (2014). Rifted continental margins: The case for depth-dependent extension. Earth Planet. Sci. Letts., 407, 148–162.

Hutchison, W., Mather, T.A., Pyle, D.M., Biggs, J., and Yirgu, G. (2015). Structural controls on fluid pathways in an active rift system: A case study of the Aluto volcanic complex. Geosphere , 11, 1-21, doi:10.1130/GES01119.1.

Isacks, B.L. (1992). Long Term Land Surface Processes: Erosion, Tectonics and Climate History in Mountain Belts. In: Mather, P. (Ed.), TERRA-1, Understanding the Terrestrial Environment. Taylor and Francis, London, UK, pp. 21e36.

Kazmin, V., Shifferaw, A., and Balcha, T. (1978). The Ethiopian basement: stratigraphy and possible manner of evolution. International Journal of Earth Sciences. Geologische Rundschau, 67, 531–546.

Kazmin, V., Seife, M.B., Nicoletti, M., and Petrucciani, C. (1980). Evolution of the northern part of the Ethiopian Rift. In: Geodynamic Evolution of the Afro-Arabian Rift System, Accademia Nazionale Dei Lincei, Atti dei Convegni Lincei, 47, 275-292.

Keir, D., Ebinger, C.J., Stuart, G.W., Daly, E., and Ayele, A. (2006). Strain accommodation by magmatism and faulting as rifting proceeds to breakup: seismicity of the northern Ethiopian rift. J. Geophys. Res..111(B5). B05314, doi: 10.1029/2005JB003748.

Keir, D., Bastow, I.D., Corti, G., Mazzarini, F., and Rooney, T.O. (2015). The origin of along-rift variations in faulting and magmatism in the Ethiopian rift. Tectonics, 34, 464-477, DOI: 10.1002/2014TC003698.

Keir, D., Bastow, I., Pagli, C., and Chambers, E. (2013). The development of extension and magmatism in the Red Sea rift of Afar. Tectonophysics, 607, 98–114.

Kendall, J.M., Stuart, G.W., Ebinger, C.J., Bastow, I.D. and Keir D. (2005). Magma assisted rifting in Ethiopia. Nature, 433**,** 146–148.

Keranen, K., and S.L. Klemperer (2008). Discontinuous and diachronous evolution of the Main Ethiopian Rift: Implications for the development of continental rifts. Earth and Planetary Science Lettters, 265, 96-111, doi:10.1016/j.epsl.2007.09.038.

Keranen, K., Klemperer, S.L., Gloaguen, R. and Eagle working group (2004). Three-dimensional seismic imaging of a protoridge axis in the Main Ethiopian rift. Geology, 32**,** 949–952.

Keranen K., Klemperer S.L., Julia J., Lawrence J.L., and Nyblade A. (2009). Low lower-crustal velocity across Ethiopia: is the Main Ethiopian Rift a narrow rift in a hot craton?. Geochem. Geophys. Geosyst., 10, Q0AB01, doi:10.1029/2008GC002293.

Kirby, E., Johnson, C., Furlong, K., and Heimsath, A. (2007). Transient channel incision along Bolinas Ridge, California: Evidence for differential rock uplift adjacent to the San Andreas fault. J. Geophys. Res. 112(F3): doi: 10.1029/2006JF000559. issn: 0148-0227.

Kirby, E., and Whipple, K. X. (2001). Quantifying differential rock-uplift rates via stream profile analysis. Geology 29, 415–418.

Kobor, J.S., and Roering, J.J. (2004). Systematic variation of bedrock channel gradients in the central Oregon Coast Range: implications for rock uplift and shallow landsliding. Geomorphology, 62: 239–256.

Kogan, L., Fisseha, S., Bendick, R., Reilinger, R., McClusky, S., King, R., and Solomon, T. (2012). Lithospheric strength and strain localization in continental extension from observations of the East African Rift.J. Geophys. Res. 117, B03402, doi:10.1029/2011JB008516.

Kooi, H. and Beaumont, C., 1994. Escarpment evolution on high-elevation rifted margins: insights derived from a surface processes model that combines diffusion, advection, and reaction. J. Geophys. Res. 99, 12191–12209.

Korme, T., Acocella, V., and Abebe, B. (2004). The role of pre-existing structures in the origin, propagation and architecture of faults in the Main Ethiopian Rift. Gondwana Research, 7, 467–479.

Laó-Dávila, D.A., Al-Salmi, H.S., Abdelsalam, M.G., and Atekwana, E.A. (2015). Hierarchical segmentation of the Malawi Rift: The influence of inherited lithospheric heterogeneity and kinematics in the evolution of continental rifts. Tectonics, 34, 2399-2417, doi:10.1002/2015TC003953.

Lock, J., Kelsey, H., Furlong, K., and Woolace, A. (2006). Late Neogene and Quaternary landscape evolution of the Northern California Coast Ranges: evidence for Mendocino triple junction tectonics. Geol. Soc. Am. Bull. 118, 1232–1246.

Mohr, P. (1962). The Ethiopian Rift System. Bulletin of the Geophysical Observatory of Addis Ababa, 5, 33-62.

Mackenzie, G.H., Thybo, G.H., and Maguire, P. (2005). Crustal velocity structure across the Main Ethiopian Rift: results from 2-dimenional wide-angle seismic modeling. Geophys. J. Int., 162**,** 994–1006.

Maguire, P.K.H., Keller, G.R., Klemperer, S.L., Mackenzie, G.D., Keranen K., Harder, S., O'Reilly B., Thybo H., Asfaw, L., Khan M.A., and Amha M. (2006). Crustal structure of the Northern Main Ethiopian Rift from the EAGLE controlled source survey; a snapshot of incipient lithospheric break-up. In: Yirgu G., Ebinger C.J., Maguire P.K.H., (Eds), 2006. The Afar Volcanic Province within the East African Rift System. Geol. Soc. Spec. Pub., 259, 269-291.

Mohr, P. (1962). The Ethiopian Rift System. Bulletin of the Geophysical Observatory of Addis Ababa, 5, 33-62.

Mohr, P. (1983). Volcanotectonic aspects of the Ethiopian Rift evolution, Bulletin Centre Recherches Elf Aquitaine Exploration Production, 7, 175-189.

Molin, P. and Corti, G. (2015). Topography, river network and recent fault activity at the margins of the central main Ethiopian rift (East Africa). Tectonophysics, 664, 67e82. http://dx.doi.org/10.1016/j.tecto.2015.08.045.

Molin, P., Pazzaglia, F.J., and Dramis, F. (2004). Geomorphic expression of active tectonics in a rapidly deforming forearc, Sila Massif, Calabria, southern Italy. Am. J. Sci. 304, 559–589.

Molnar, P., and England, P. (1990). Late Cenozoic uplift of mountain ranges and global climate change: chicken or egg?. Nature, 346(6279), 29-34.

Pazzaglia, F. J., and Gardner, T. W. (1994). Late Cenozoic flexural deformation of the middle US Atlantic passive margin. J. Geophys. Res.: Solid Earth, 99(B6), 12143-12157.

Pazzaglia, F.J., Gardner, T.W., and Merritts, D.J. (1998). Bedrock Fluvial Incision and LongitudinalProfile Development over Geologic Time Scales Determined by Fluvial Terraces. In: Wohl, E., Tinkler, K. (Eds.), River Over Rock: Fluvial Processes in Bedrock Channels American Geophysical Union Geophysical Monograph 107. American Geophysical Union, Washington, DC, pp. 207–235.

Pérez-Gussinyé M., Metois M., Fernández M., Vergés J., Fullea J., and Lowry A.R. (2009). Effective elastic thickness of Africa and its relationship to other proxies for lithospheric structure and surface tectonics. Earth Planet. Sci. Letts., 287, 152-167

Petit, C., Fournier, M. and Gunnell, Y. (2007). Tectonic and climatic controls on rift escarpments: Erosion and flexural rebound of the Dhofar passive margin (Gulf of Aden, Oman). J. Geophys. Res., 112, B03406, doi:10.1029/2006JB004554

Philippon, M., Corti, G., Sani, F., Bonini, M., Balestrieri, M.L., Molin, P., Willingshofer, E., Sokoutis, D., and Cloetingh, S. (2014). Evolution, distribution and characteristics of rifting in southern Ethiopia. Tectonics 33, 485-508, doi:10.1002/2013TC003430.

Pik, R., Marty, B., Carignan, J., Yirgu, G., and Ayalew, T. (2008). Timing of East African Rift development in southern Ethiopia: Implication for mantle plume activity and evolution of topography. Geology, 36(2), 167-170. doi: 10.1130/G24233A.1

Pizzi, A., Coltorti, M., Abebe, B., Disperati, L., Sacchi, G., and Salvini, R. (2006). The Wonji fault belt (Main Ethiopian Rift): Structural and geomorphological constraints and GPS monitoring. In The Afar Volcanic Province Within the East African Rift System, edited by G. Yirgu, C. J. Ebinger, and P. K. H. Maguire, Geol. Soc. Spec. Pub. 259, 191–207.

Ponza, A., Pazzaglia, F.J., and Picotti, V. (2010). Thrust-fold activity at the mountain front of the Northern Apennines (Italy) from quantitative landscape analysis. Geomorphology123, 211–231.

Ring, U. (1994), The influence of preexisting structure on the evolution of the Cenozoic Malawi Rift (East African Rift System), Tectonics, 13, 313-326.

Ritsema, J., van Heijst, H.J., and Woodhouse, J.H. (1999). Complex shear wave velocity structure imaged beneath Africa and Iceland. Science 286, 1925–1928.

Rooney, T. O. (2010). Geochemical evidence of lithospheric thinning in the southern Main Ethiopian Rift. Lithos, 117(1), 33-48.

Rowland, J. V., Baker, E., Ebinger, C. J., Keir, D., Kidane, T., Biggs, J., ... and Wright, T. J. (2007). Fault growth at a nascent slow-spreading ridge: 2005 Dabbahu rifting episode, Afar. Geophys. J. Int., 171(3), 1226-1246.

Saria, E., Calais, E., Stamps, D. S., Delvaux, D., and Hartnady, C. J. H. (2014). Present-day kinematics of the East African Rift, J. Geophys. Res., 119, 3584–3600, doi: 10.1002/2013JB010901

Scholz, C.H. and J. C. Contreras (1998), Mechanics of continental rift architecture, Geology, 26, 967-970.

Schorghofer, N. and Rothman, D.H. (2002). A causal relations between topographic slope and drainage area. Geophys. Res. Lett. 29. http://dx.doi.org/10.1029/2002GL015144.

Scotti, V.N., Molin, P., Faccenna, C., Soligo, M., and Casas-Sainz, A. (2013). The influence of surface and tectonic processes on landscape evolution of the Iberian Chain (Spain): quantitative geomorphological analysis and geochronology. Geomorphology http://dx.doi.org/10.1016/j.geomorph.2013.09.017.

Sembroni, A., Molin, P., Pazzaglia, F.J., Faccenna, C., and Bekele, A. (2016a). Evolution of continental-scale drainage in response to mantle dynamics and surface processes: an example from the Ethiopian Highlands. Geomorphology 261, 12e29.http://dx.doi.org/10.1016/j.geomorph.2016.02.022.

Sembroni, A., Faccenna, C., Becker, T.W., Molin, P., and Bekele, A. (2016b). Long term, deep mantle support of the Ethiopia-Yemen Plateau. Tectonics 35, 469e488. http://dx.doi.org/10.1002/2015TC004000.

Sklar, L.S. and Dietrich, W.E. (1998). River Longitudinal Profiles and Bedrock Incision Models: Stream Power and the Influence of Sediment Supply. In: Tinkler, K., Wohl, E.E.(Eds.), Rivers Over Rock: Fluvial Processes in Bedrock Channels. American Geophysical Union Geophysical Monograph 107, pp. 237–260.

Snyder, N., Whipple, K. X., Tucker, G. E., and Merritts, D. J. (2000). Landscape response to tectonic forcing: Digital elevation model analysis of stream profiles in the Mendocino triple junction region, northern California. Geol. Soc. Am. Bull.112 (8), 1250-1263.

Sokoutis D., Corti G., Bonini M., Brun J.-P., Cloetingh S. Mauduit T., and Manetti P. (2007). Modelling the extension of heterogeneous hot lithosphere. Tectonophysics, 444, 63-79.

Stern, R.J. (2002). Crustal evolution in the East African Orogen: a neodymium isotopic perspective. J. Afri. Earth Sci., 34, 109-117.

Stern, R.J., K.C. Nielsen, E. Best, M. Sultan, R.E. Arvidson, and A. Kroner (1990). Orientation of the late Precambrian sutures in the Arabian-Nubian Shield. Geology, 18, 1103-1106.

Stern, T. A., Baxter, A. K., and Barrett, P. J. (2005). Isostatic rebound due to glacial erosion within the Transantarctic Mountains. Geology, 33(3), 221-224.

Stuart, G.W., Bastow, I.D., and Ebinger, C.J. (2006). Crustal structure of the northern Main Ethiopian Rift from receiver function studies. In: Yirgu G., Ebinger C.J., Maguire P.K.H., (Eds), 2006. The Afar Volcanic Province within the East African Rift System. Geol. Soc. Spec. Pub., 259, 253-267.

Tarboton, D. G., Bras, R. L., and Rodríguez-Iturbe, I. (1989). Scaling and elevation in river networks. Water Resources Research 25, 2037–2051.

Tomkin, J.H., Brandon, M.T., Pazzaglia, F.J., Barbour, J.R., and Willett, S.D. (2003). Quantitative testing of bedrock incision models, Clearwater River, NW Washington State. J. Geophys. Res. 108 (B6). http://dx.doi.org/10.1029/2001JB000862.

Tommasi, A., and Vauchez, A. (2001). Continental rifting parallel to ancient collisional belts: an effect of the mechanical anisotropy of the lithospheric mantle. Earth Planet. Sci. Letts., 185, 199-210.

Trippanera, D., Ruch, J., Acocella, V., and Rivalta, E. (2015a). Experiments of dike-induced deformation: Insights on the long-term evolution of divergent plate boundaries. J. Geophys. Res.: Solid Earth, 120(10), 6913-6942.

Trippanera, D., Acocella, V., Ruch, J., and Abebe, B. (2015b). Fault and graben growth along active magmatic divergent plate boundaries in Iceland and Ethiopia. Tectonics, 34(11), 2318-2348.

Tucker, G. E. and Slingerland, R. L. (1994). Erosional dynamics, flexural isostasy, and long-lived escarpments: A numerical modeling study. J. Geophys. Res.: Solid Earth, 99(B6), 12229-12243.

Vail, J.R. (1985). Pan-African crustal accretion in north-east Africa. Journal African Earth Sciences, 1, 285–294, 1983.

Vauchez, A., Barruol G., and Tommasi, A. (1997). Why do continents break‐up parallel to ancient orogenic belts?. Terra Nova, 9, 62-66.

Versfelt, J., and Rosendahl, B. R. (1989). Relationships between pre-rift structure and rift architecture in Lakes Tanganyika and Malawi: East Africa. Nature, 337, 354-357.

Wegmann, K.W. and Pazzaglia, F.J. (2002). Holocene strath terraces, climate change, and active tectonics: the Clearwater River basin, Olympic Peninsula, Washington State. Geol. Soc. Am. Bull. 114, 731–744.

Weissel, J. K. and Karner, G. D. (1989), Flexural uplift of rift flanks due to mechanical unloading of the lithosphere during extension, J. Geophys. Res., 94, 13,919–13,950, doi:10.1029/JB094iB10p13919

Weissel, J., Malinverno, A., and Harding, D. (1995). Erosional development of the Ethiopian Plateau of Northeast Africa from fractal analysis of topography. In: Barton, C.C., Pointe,P.R. (Eds.), Fractals in Petroleum Geology and Earth Processes. Plenum Press, NewYork, pp. 127–142.

Wernicke, B. (1985). Uniform-sense simple shear of the continental lithosphere, Can. J. Earth Sci., 32, 108-125.

Whaler, K.A. and Hautot, S. (2006). The electrical resistivity structure of the crust beneath the northern Main Ethiopian Rift. In: Yirgu G., Ebinger C.J., Maguire P.K.H., (Eds), 2006. The Afar Volcanic Province within the East African Rift System. Geol. Soc. Spec. Pub., 259, 293-305.

Whipple, K.X., Hancock, G.S., and Anderson, R.S. (2000). River incision into bedrock: mechanicsand relative efficacy of plucking, abrasion, and cavitation. Geol. Soc. Am. Bull. 112,490–503.

Whipple, K. X. (2004). Bedrock rivers and the geomorphology of active orogens. Annual Review of Earth and Planetary Sciences 32, 151-185.

Whipple, K. X. and Tucker, G. E. (1999). Dynamics of the stream-power river incision model: implications for height limits of mountain ranges, landscape response timescales, and research needs. J. Geophys. Res. 104, 17,661-17,674.

Whipple, K.X., Wobus, C., Crosby, B., Kirby, E., and Sheehan, D. (2007). New Tools for Quantitative Geomorphology: Extraction and Interpretation of Stream Profiles from Digital Topographic Data. Geological Society of America Annual Meeting, Short Course Guide: http://www.geomorphtools.org, Denver.

Wittmann, H., von Blanckenburg, F., Kruesmann, T., Norton, K. P., and Kubik, P. W. (2007). Relation between rock uplift and denudation from cosmogenic nuclides in river sediment in the Central Alps of Switzerland. J. Geophys. Res., 112(F4).

Wobus, C., Whipple, K. X., Kirby, E., Snyder, N., Johnson, J., Spyropolou, K., Crosby, B., and Sheehan, D. (2006). Tectonics from topography: Procedures, promise, and pitfalls. In: Willett, S., Hovius, N., Brandon, M.T, Fisher, D.M. (Eds), Tectonics, Climate, and Landscape Evolution. Geol. Soc. Am. Spec. Pap., 398, 55 –74.

WoldeGabriel, G., Aronson, J. L., and Walter, R. C. (1990). Geology, geochronology, and rift basin development in the central sector of the Main Ethiopia Rift. Geological Society America Bulletin102, 439-458.

Wolfenden, E., Ebinger, C., Yirgu, G., Deino, A., and Ayale, D. (2004). Evolution of the northern Main Ethiopian rift: birth of a triple junction. Earth Planet. Sci. Letts. 224, 213–228.

Ziegler, P. A. and S. Cloetingh (2004), Dynamic processes controlling evolution of rifted basins, Earth-Sci. Rev., 64(1–2), 1–50, doi:10.1016/S0012-8252(03)00041-2.

Table 1. Summary of the characteristics of the different MER sectors (see text for further details)

Sector	Length (km)	Structure	Main Border Fault	Active deformation	Magmatic activity	Rift margin elevation drop (m)		Topography gradient of rift margin	
						West	East	West	East
1	70	Symmetric	-	Mostly axial (minor activity in the Western margin)	Axial (Wonji)	1799	1750	0.047	0.040
2	100	Asymmetric	East	Axial	Axial (Wonji)	1500	1416	0.019	0.042
3	50	Asymmetric	West	Marginal	Marginal (Wonji+SDZ)	1392	870	0.058	0.029
4	60	Symmetric	-	Mostly marginal (axial subordinate)	Axial (WFB)	946	897	0.019	0.027
5	100	Asymmetric	East	Marginal (activity at the Western margin)	Marginal (mixed Wonji+SDZ characteristics)	665	948	0.019	0.067
6	120	Symmetric (Chamo basin) Asymmetric (Galana basin, Gofa Province)	East and West	Mostly marginal (axial subordinate)	Almost absent	1164.8 (Chamo basin)	1248.2 (Chamo basin)	0.042 (Chamo basin)	0.037 (Chamo basin)

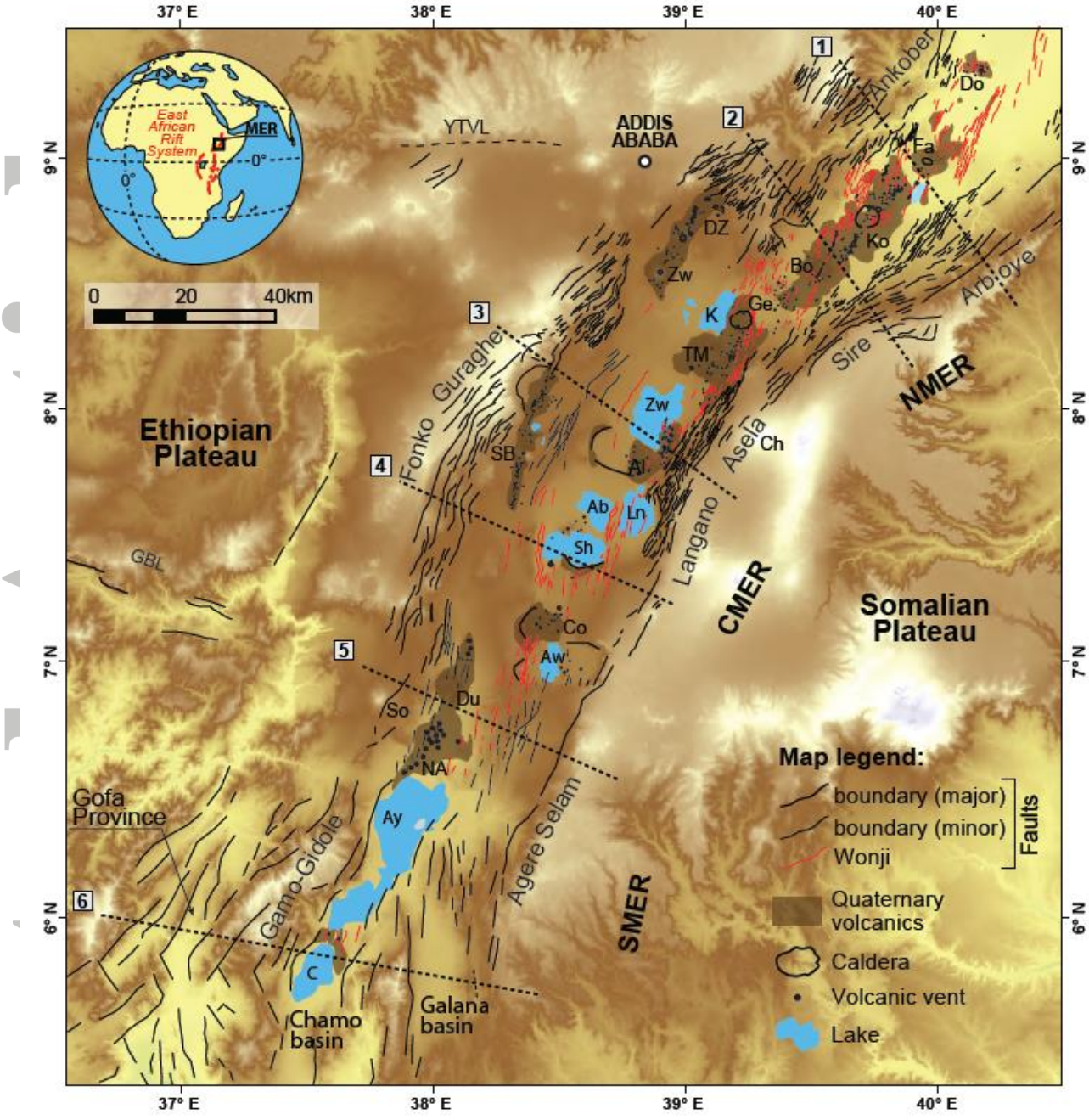

Figure 1. Fault pattern and Quaternary volcanics in the Main Ethiopian Rift (MER) superimposed on a NASA's Shuttle Radar Topography Mission (SRTM) digital elevation model. The three main rift sectors are labelled as: NMER, Northern MER; CMER, Central MER; SMER, Southern MER. Dashed lines with numbers indicate the cross-sections illustrated in Fig. 2. Volcanic fields and calderas are labelled as follows: Al: Aluto; Bo, Boseti; Co, Corbetti; Do, Dofan; Du, Duguna; DZ, Debre Zeyt; Fa, Fantale; Ge, Gedemsa; Ko, Kone; NA, North Abaya; SB, Silti-Butajira; TM, Tulu Moye; Zw, Zikwala. Lakes labelled as follows: Ab, Lake Abijata; Ay, Abaya; Aw, Awasa; C, Lake Chamo; Ch: Chilalo;

K, Lake Koka; Ln, Langano; Sh, Shala; Zw, Lake Ziway. Other labels: GBL: Goba-Bonga transversal lineament; So: Soddo; YTVL: Yerer-Tullu Wellel volcano-tectonic lineament.

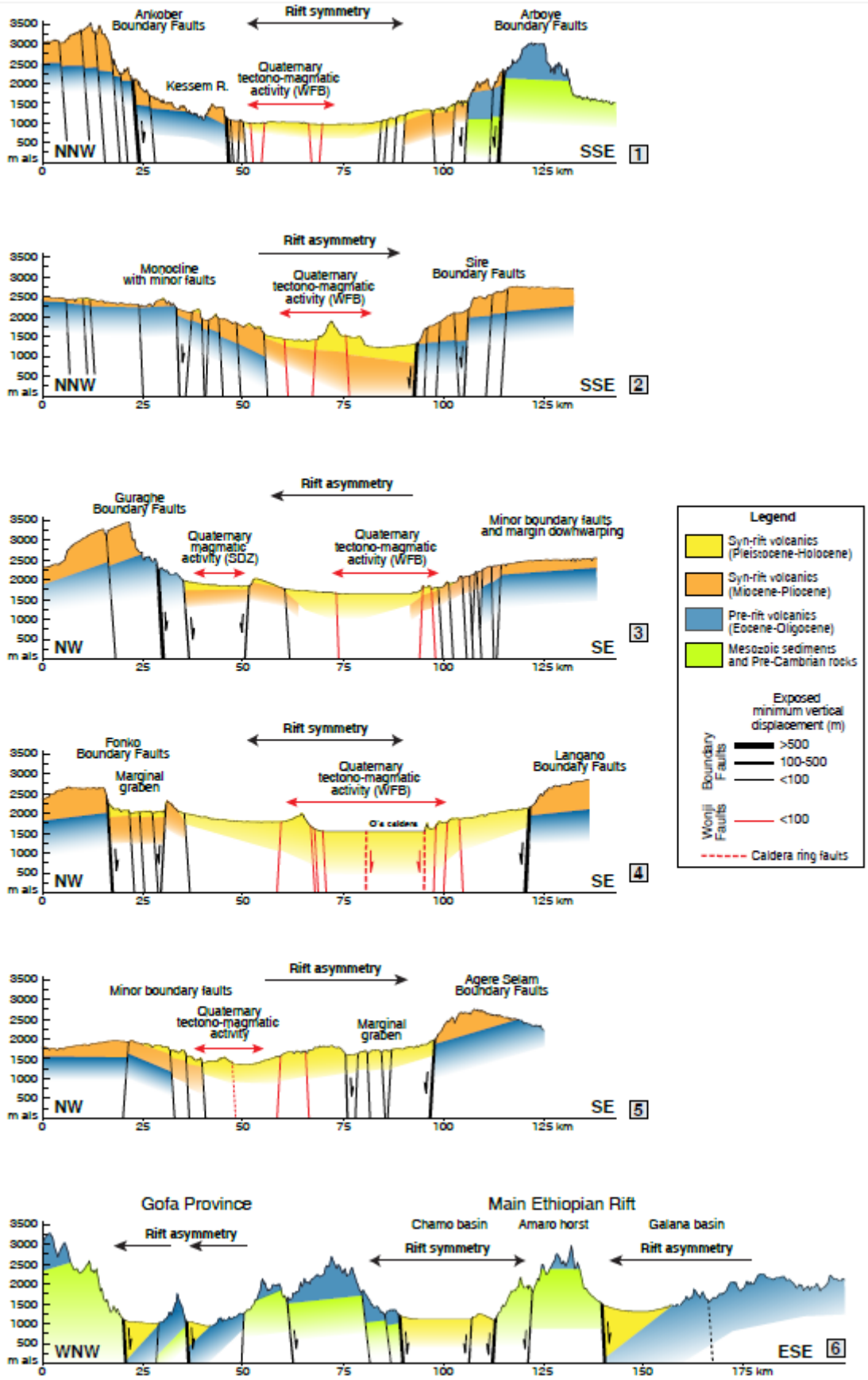

Figure 2. Simplified geological profiles across different sectors of the MER. Topographic profiles are extracted from SRTM digital elevation models, with vertical exaggeration of 10.

WFB: Wonji Fault Belt; SDZ: Silti Debre Zeit volcanic belt. Sources for the geological profiles: Abebe et al. (2005); Agostini et al. (2011a); Corti et al. (2013); Davidson (1983); Ebinger et al. (1993, 2000); Ethiopian Mapping Agency (1978, 1981); Ethiopian Mapping Authority (1996); Hutchison et al. (2015); Philippon et al. (2014); Wolfenden et al. (2004).

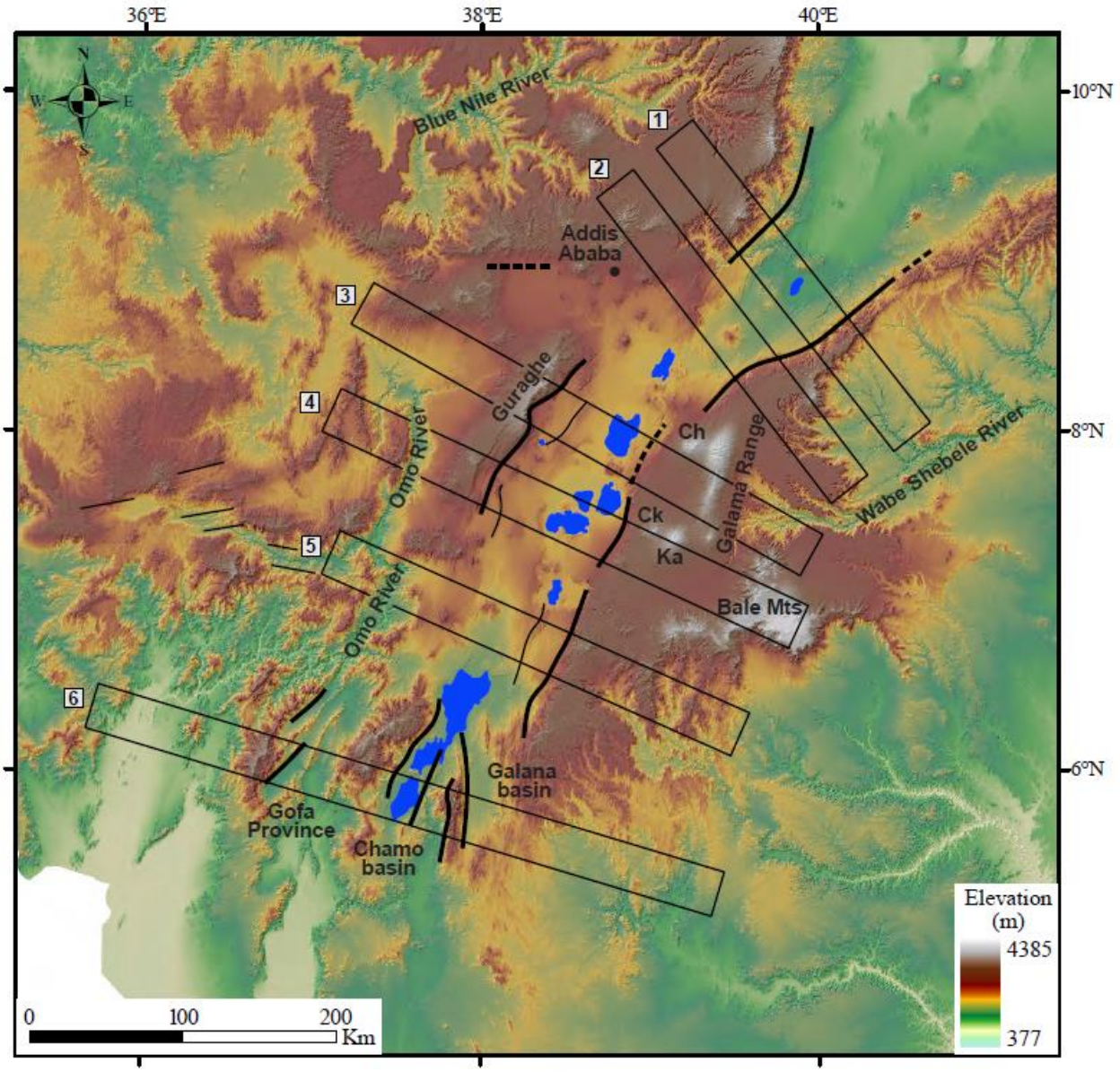

Figure 3. Topography of the study area (SRTM digital elevation model, 90 m of resolution) including the main tectonic structures (solid and dashed lines) and the swath profiles location. Ch: Mt Chilalo; Ck: Mt Chilke; Ka: Mt Kaka.

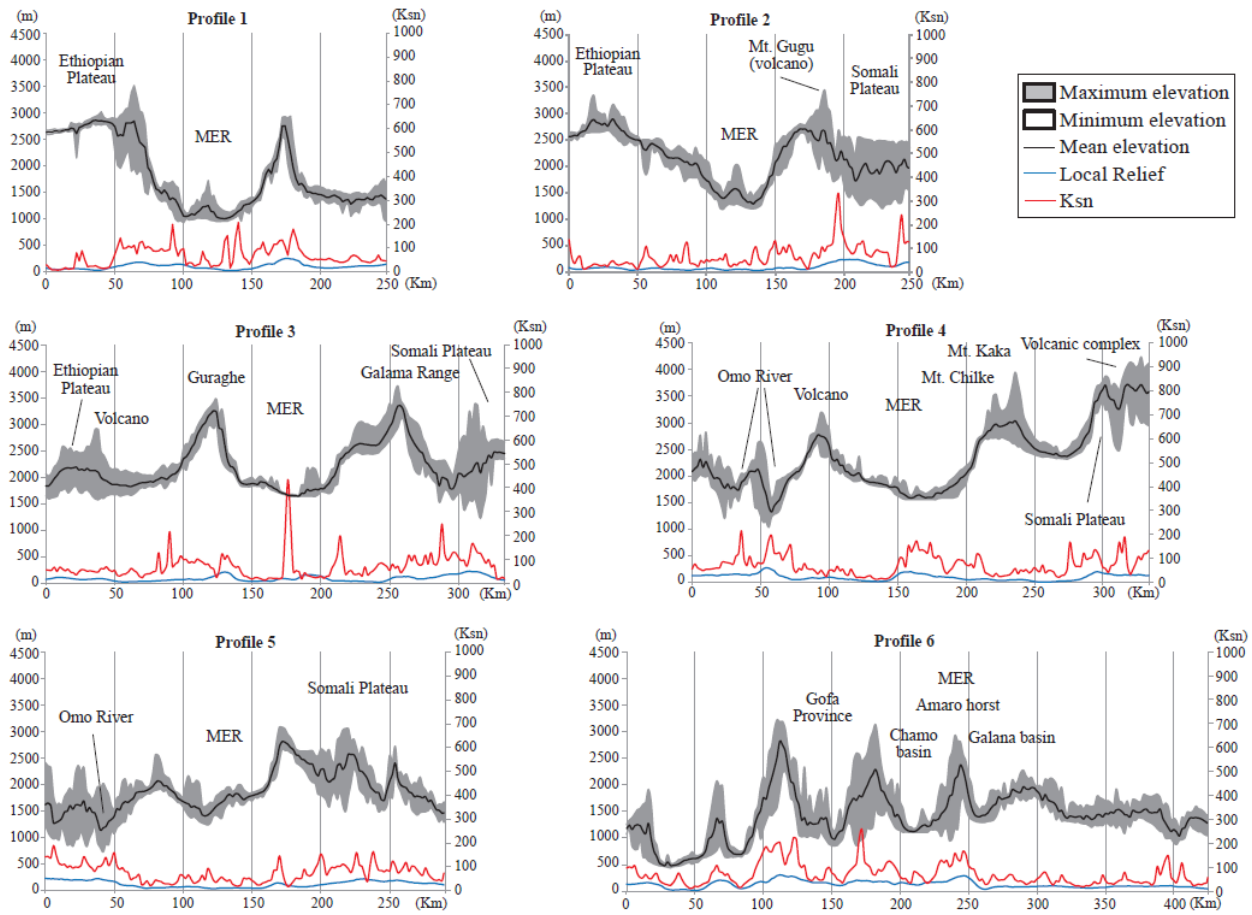

Figure 4. Swath profiles illustrating the maximum, mean, and minimum elevation pattern cutting across the MER. The plots include also the variation in the mean values of local relief and channel steepness index (see text for explanation and Fig. 5 for profiles location).

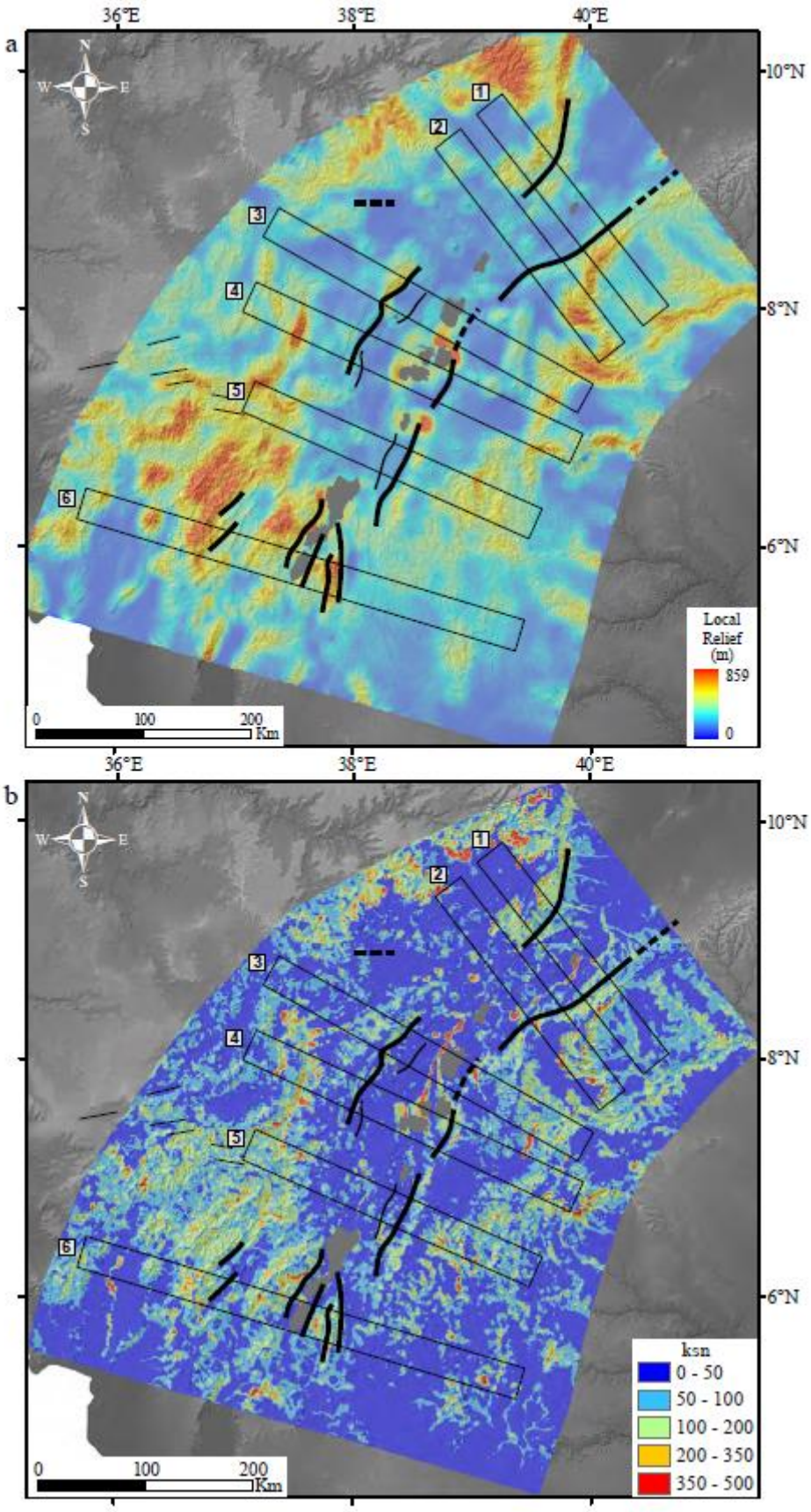

Figure 5. a) Map of the local relief of the study area: note how the correspondence between high values of local relief at the rift margins and location of the main structures evidences the

symmetry/asymmetry of the MER sectors. b) Map of the along channel variation of the steepness index: along the rift margins high values of channel steepness correspond with the main tectonic structures.

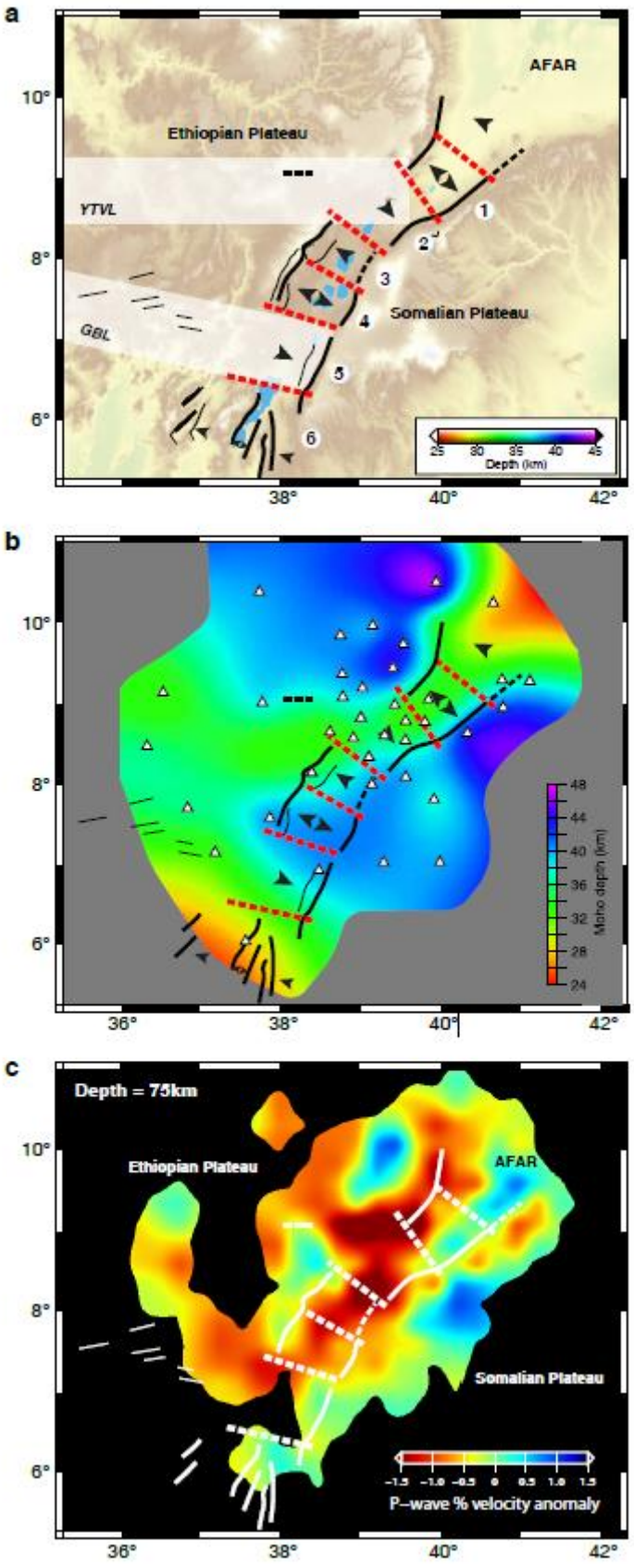

Figure 6. a) Interpreted along-axis variations in the structure of the Main Ethiopian Rift. Single arrows indicate the polarity of the different rift sectors; double arrows indicate

symmetry of rifting. Whitish boxes indicate the hypothesised extent of the transversal YTVL: Yerer-Tullu Wellel (YTWL) and Goba-Bonga (GBL) volcano-tectonic lineaments. b) Contour map of Moho depth in the MER (after Keranen et al., 2009). c) Depth slices through the P wave velocity model of Bastow et al. (2008) at 75 km depth. See text for further details.